

IHTC15-09262

HEAT TRANSFER CHARACTERISTICS IN FORCED CONVECTION THROUGH A RECTANGULAR CHANNEL WITH V-SHAPED RIB ROUGHENED SURFACES

D. Fustinoni, P. Gramazio, L.P.M. Colombo, A. Niro*

Politecnico di Milano, Department of Energy, Campus Bovisa, via Lambruschini, 4 – 20156 Milano, Italy

ABSTRACT

In this paper we present experimental results for a channel with the lower and upper surfaces with V-shaped ribs pointing upward. The duct cross-section is 120-mm wide and 12-mm height, and the channel is operated with the lower and upper walls at fixed temperature whereas sides are adiabatic. The ribs have square cross section of 2 mm in side, a V-apex angle of 60°, and three pitch-to-side ratios (10, 20, 40); finally, they are in-line arranged on the two walls. Air flow-rates have been varied in order to investigate Reynolds numbers, based on the duct hydraulic diameter, between 700 and 7500. Data in a similar channel but with flat surfaces have been collected for comparison as well. The data show that the flow regime seems to be turbulent even at the lowest tested value of Re; the friction factor displays the typical trend for k-roughened surfaces, i.e., it becomes independent of Re for sufficiently high values of Re. The dependence of the Nusselt number on the Reynolds number and the pitch-to-side ratio is presented in the form of a power law correlation. Various figures of performance have been evaluated, showing that for Re>1300 the adoption of the ribbed surface is always advantageous and allows a maximum heat transfer enhancement factor between 2.5 and 4, decreasing with the pitch-to-side ratio.

KEY WORDS: Convection, heat transfer enhancement, heat exchanger, rectangular channel, cooling turbine blade, V-shaped ribs

1. INTRODUCTION

Heat transfer in forced convection inside rectangular channels is a very interesting matter for industry as it is encountered in critical heat transfer applications like gas-turbine blade cooling [1], and in devices largely used such as plate-fin compact heat exchangers. In designing these devices, high values of heat transfer area per unit volume are searched for; however, if this parameter is increased over a given value, thermal performances start worsening. In fact, the higher the surface-to-volume ratio the narrower the passages, so air velocity has to be lowered to maintain acceptable the pressure drops; however, narrow passages and low air velocities lead to laminar flows laminarization that is of course characterized by a rather poor convective coefficient which eventually defeats completely the area increase benefits. To overcome this limit, heat transfer is enhanced by configuring surfaces with a large variety of fins and ribs, which are an efficient and cost-effective solution. The literature review shows that, starting from the '70s, a continuously growing number of studies have been dealing with heat transfer over rib-roughened surfaces.

A first crucial feature for this kind of roughness is the rib arrangement with respect to the main stream. The number of possible configurations, indeed, is very large but four arrangements have been particularly considered so far in literature, namely, transverse-, parallel-tilted-, cross-inclined- and V-shaped-ribs; in addition, ribs may be assembled on the opposite walls either staggered or in-line. In this paper, we focus particularly on the parallel-tilted and cross-tilted arrangements. A brief discussion of relevant works in literature is presented below making use of the following dimensionless geometric parameters: the channel aspect ratio AR, i.e., the base to height ratio (making reference to the channel cross section), the dimensionless pitch p/e, i.e., the pitch to rib height ratio, and the blockage factor e/D_h defined as the rib height to the channel hydraulic diameter ratio.

*Corresponding Author: alfonso.niro@polimi.it

1.1 Parallel-tilted ribs The first major studies were carried out starting from the first half of the '80s by Han [2-7], Park [8], and Kukreja [9]. It was observed that tilting the ribs with respect to the main flow direction results in higher heat transfer performance due to the presence of secondary flows. Actually, as a consequence of inclination, two counter-rotating vortices develop near the rib and slide along it. They interact with the main flow carrying part of the colder core towards the wall. Furthermore, the interaction between main and secondary flows affects the reattachment point, and hence the recirculation-zone between two successive ribs. Specifically, a great deal of work was devoted to the case with a tilt angle α =45°; it was found that the optimum dimensionless pitch p/e strongly depends on both e/D_h and AR. The most studied configuration presents AR=1 with all the sides heated.

Among the recent studies, there are the papers of Liu et al. [10] [11], Choi et al. [12], and Smulsky et al. [13]. Liu et al. [10] [11] carried out experiments on heat transfer characteristics in steam-cooled rectangular channels with parallel-tilted ribs on the opposite walls, for two tilt angles, i.e., 45° and 60° , several aspect ratios within 0.5 and 2.0, and Reynolds number ranging from 10000 to 140000. They found that thermal performances for α =45° are 15-25% larger than for α =60°. They also showed that heat transfer coefficients for steam are 12-25% higher than for air.

Choi et al. [12] studied the local heat transfer characteristics on two kinds of surfaces, namely, smooth or dimpled, with parallel-tilted ribs (α =60°). They found that ribs are more effective than dimples in enhancing heat transfer. Smulsky et al. [13] investigated the effect of different tilt angles of a single rib on a smooth surface. The local heat transfer maximum for 50° is approximately 40% higher than that for 90°, while its position depends on rib side dimension.

Tanda in [14] focuses on the effect of rib spacing on the thermal performance, testing configurations with a tilt angle α =45° and four different p/e: 6.66, 10, 13.33, and 20. This work shows that the largest increase of the heat transfer coefficient occurs for the single-ribbed wall channel with p/e = 13.33, where the Nusselt number ratio (Nu/Nu₀) varies from 1.85 to 2.25 (with Reynolds number decreasing), and for the two-ribbed wall channel with p/e = 10, in which the Nusselt number ratio varies from 2.1 to 2.55 (with Reynolds number decreasing).

1.2. Cross-tilted and V-shaped From the '90s some studies, for instance those of Han et al. [7], and Won and Ligrani [15], have been devoted to cross-tilted configurations aiming at enhancing the effect of secondary flows. Both these papers pointed out that thermal performances are not as high as expected. In [7] the cross-tilted arrangement displays the smallest pressure drop penalty but heat transfer enhancement is so low that the authors did not recommend this arrangement for turbine blade cooling.

Krukeja et al. [9], Gao and Sunden [16] use V-shaped ribs, another ribs arrangement in order to enhance the effect of secondary flows. In particular, V-shaped ribs may present the apex upward or downward the main flow direction. In the former arrangement, secondary flows move from the center to the lateral sides of the channel, whereas in the latter the situation is reversed. It has not been yet assessed which configuration is the best in enhancing heat transfer, because controversial results have been found, probably due to the different boundary conditions taken into consideration.

Finally, in the last decade, rectangular channels with only one heated, ribbed surface have aroused great interest for applications in renewable energy technologies as solar air heaters, for example Tanda [17]. Reviews on this subject are reported in Bhushan and Singh [18], Hans et al. [19] and Patil et al. [20].

A closer look reveals that most of the work done up to now focused on fully turbulent flow regimes. Moreover, two aspects are very little investigated, namely, the impact of high values of the blockage factor, and the laminar-to-turbulent flow regime transition. Both these aspects are very relevant in designing compact heat exchangers, as well shown by the specific literature [21]. For this reason we started an experimental campaign aimed at investigating heat transfer coefficients and pressure drops in rectangular ducts with variously arranged square ribs, in a range of Reynolds numbers between 600 and 8000. In these conditions, it is possible to explore both the turbulence onset and the transition region. In this paper we present a selection of the available results while experimental runs are under completion.

2. EXPERIMENTAL SETUP

As schematically shown in figure 1(a), the experimental setup consists of two independent circuits, namely, the air-circuit containing the test section, and the heating-water circuit used to control the temperature of the channel walls.



Fig. 1 Schematics of the experimental setup: 1. fine mesh screen cover; 2. convergent air inlet; 3. entry-section; 4. test-section; 5. exit-section; 6. rotameters; 7. by-pass; 8. blower; 9. heat bath; 10. water circuit piping (a), test section with the duct on the wall backside (b)

Through a convergent, room air flows into the circuit; a fine mesh screen covers the convergent inlet whereas at its outlet there is a flow straightener consisting in a matrix of staggered 4-mm-diameter, 40-mm long thin polystyrene tubes. Inside the convergent a thermo-resistance, i.e., a resistance thermometer, is mounted to measure the air temperature. From the straightener air flows into an entry-section that is a rectangular duct with the same cross dimensions as the tested channel; entry-section is 0.8-m long, i.e., near 40 times the channel hydraulic diameter, and its walls are made with 10-mm thick plexiglas plates and are not heated. At the end of this section, air enters the test-section that is a 120-mm wide, 12-mm height, 880-mm long duct; its lower and upper walls are two aluminum plates of 10-mm minimum thickness with a rib configured face.

As shown in figure 1(b), the backside of each plate is covered by a cap strongly tightened to the plate, so that they form a jacket where the heating water flows. Inside and outside the water jacket there are ribs which prevent the plate buckling. To check if temperature is uniform over the heated walls, four thermocouples are embedded in the lower wall, and three in the upper one; each thermocouple is cemented into a 1.8-mm-wide, 0.5-mm-depth groove cut in the flat face; thermocouple locations are displayed in figure 2 whereas table 1 lists the exact position of their junctions. Eventually, the test-section sides are closed by 4-mm-thick glass plates to allow optical access inside the channel.

At the test-section outlet, there is a short exit-section equipped with two turbolizer rows followed by a convergent that conveys air through a 20-mm-wide, 6-mm-high channel partially filled by a fine-meshed plastic net; after the screen, a PTR and a thermocouple are positioned on the centerline of this channel to measure the air bulk-temperature. Finally, inside the couplings between the entry-section and the test-section, and between this one and the exit-section there are two pressure taps, each consisting in a 1.5-mm-diameter hole (great care was devoted in eliminating any burr). Downstream the exit-section there are three rotameters, i.e., float-type flow-meters, connected in parallel with full scale of 6, 23.5 and 40 m³/h respectively, a metering valve, and a 7-stage, 30-kPa-head, 5.5-kW-power blower operating in suction mode. The exhausted air is discharged outside the laboratory. Air temperature is also measured upstream the flow-meters by means of a thermocouple plugged in the pipe.

Table 1 Probe positions on ribbed channel wall.

Upper wall		Lower wall		
x (mm)	y (mm)	x (mm)	y (mm)	
120	60	70	60	
440	60	120	60	
760	60	440	60	
		760	60	

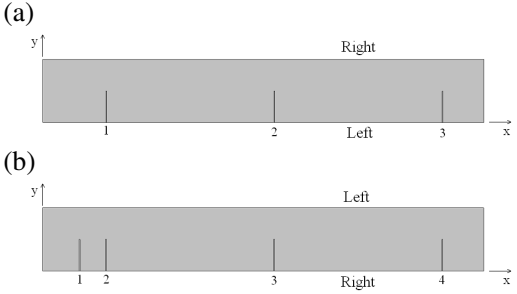


Fig 2 Thermocouples locations on upper (a) and lower (b) test channel walls.

The heating circuit is mainly composed by a heat bath which provides high mass flow-rate of water at constant temperature, and by the channels built into the upper and lower test-section walls (water and air stream in counterflow); two thermocouples are placed inside each water channel, near the entry and exit ports, respectively. The heat bath is the ThermoHaake B12 with a tank of 12-dm³, a 3-kW heater and a high precision controller; water temperature inside the tank is kept constant within 0.01 K.

3. MEASUREMENTS, DATA PROCESSING AND ERROR ANALYSIS

The thermocouples used are T-type with 0.5-mm-diameter wires, whereas the PTR are 4-wires, 100-ohm, Platinum type, i.e., PT100, with dimensions of 2 mm x 4 mm. Both thermocouples and thermo-resistances were all preliminary calibrated over five points within the temperature range from 22 to 60 °C, by means of the ThermoHaake heat bath. The probes were immersed all together into the bath while devoting great care in their positioning; for each calibration point, 160 readings per probe were collected; the resulting standard deviation is of 0.02 K for the thermocouples, and of 0.01 K for the thermo-resistances. All temperature measurements are performed by means of an Agilent 34970A data logger equipped with a relay multiplexer and a 6½ digit multimeter. The channels are sequentially read, by waiting a 0.5-s settling time after each channel-locking, with an integration time of 400 ms which ensures a standard deviation of 0.01 K that is less than or equal to the probe uncertainties; consequently, reading cycles are performed every 20 s. Pressure drops are measured by connecting the two pressure taps, placed at the inlet and outlet of the test channel, to a differential micromanometer with a full scale of 250 Pa and a 0.125-Pa sensitivity. Air volume-flow-rate is measured by means of the aforementioned rotameters which have a 2% nominal accuracy; however, by means of a calibration performed by measuring pressure drops of laminar air-flows through a smooth circular tube, we found that their accuracy is better of 1%. Finally, in order to guarantee repeatability to measurements, we adopted a precise test procedures described in the following. First, we power the bath heater and water starts to circulate through the entire circuit included the ducts on the test-section wall backside. After 30 min, that is the time to stabilize the channel wall temperature to a prefixed value within a 0.01-K band, we power the blower and air starts to flow through the test section. Then we need to wait for other 30 min in order to attain regime conditions with all temperature timefluctuations within 0.02-K band; in this conditions, channel wall-temperature is uniform within 0.1 K over the entire heated length. Eventually, we start to collect 20 reading-cycles which take 400 s; during this time, measurements of the air-volume-flow-rate and of reading-cycles was chosen first by collecting data for N=200 for some of the most representative regime conditions, and then by calculating their average standard deviation as a function of N; as a result, we found that at N=20 the average standard deviation becomes less than 0.01 K, and thus we assumed that 20 is the minimum reading-cycle number to be collected.

The average Nusselt over the test section and the Darcy-Weisbach friction factor are calculated as follows

$$Nu = \frac{hD_h}{k} = \frac{\dot{Q}/A_S}{\Delta T_{m,Log}} \frac{D_h}{k} = \frac{\dot{m}c_p(\theta_i - \theta_o)}{A_S[(\theta_i - \theta_o)/\ln(\theta_i - \theta_o)]} \frac{D_h}{k} = \frac{D_h}{k} \frac{\rho \dot{V}c_p}{A_S} \ln \frac{\theta_i}{\theta_o}$$
(1)

$$f = \frac{\Delta p}{\rho u^2 / 2} \frac{D_h}{\ell_{taps}} = \frac{2\Delta p A^2 D_h}{\rho \dot{V}^2 \ell_{taps}}$$
 (2)

where \overline{h} the average convective coefficient, \dot{Q} the total heat power exchanged, A and A_S the cross-section area and the total heated area, respectively, of the test section, $D_h=2A/(w+h)$ the channel hydraulic diameter, $\Delta T_{m,Log}$ the log-mean-temperature difference, θ_i and θ_o the wall-to-air-bulk-temperature difference at the entrance and exit, respectively, of the test section, \dot{m} and \dot{V} the mass-flow-rate and the volume-flow-rate of air, respectively, ρ the density calculated at the temperature where \dot{V} is measured, c_p the specific heat at constant pressure and k the thermal conductivity of air, Δp the pressure drop, and ℓ_{taps} the distance between the pressure taps. The error analysis, performed according to Moffat [22], gives an uncertainty less than 3% on the average convective coefficient, and less than 7% on the Darcy-Weisbach friction factor.

4. RESULTS

Experimental results refer to a rectangular channel with V-shaped ribs pointing upward on the lower and upper surfaces as schematically shown in figure 3. Ribs have a square-cross section and are made of linden wood, i.e., a material with very low thermal conductivity, to avoid that ribs behave as fins and hence to put in evidence only the role played by fluid dynamics in enhancing heat transfer. Tests have been carried out on many configurations differing for the pitch-to-side ratio as listed in table 2, whereas channel main dimensions are listed in table 3.

Table 2 Configurations parameters.

e [mm]	p [mm]	e/D _h	p/e	e/h
2	20	0.0917	10	0.1667
2	40	0.0917	20	0.1667
2	80	0.0917	40	0.1667

Table 3 Main channel parameters.

Channel height, h	12.00 mm
Channel length, L	880.00 mm
Channel width, w	120.00 mm
Hydraulic diameter, D_h	21.82 mm
Height-to-width ratio	0.10

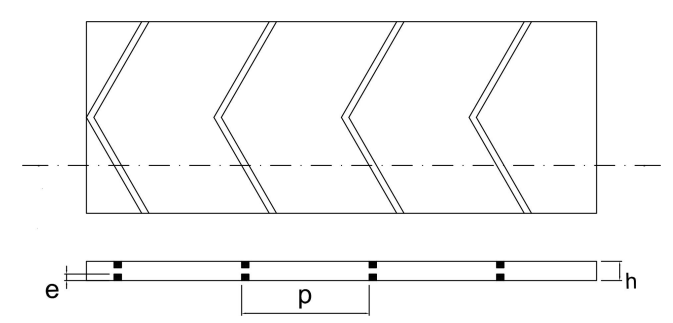


Fig. 3 Typical configuration of the V-shaped ribbed suface.

All data refer to fixed and uniform wall channel temperature at the nominal value of 40°C, and for air-flows entering into the test-section at room temperature of 22°C on average (elaborations, indeed, account for the local values).

Figure 4a shows the average Nusselt number plotted versus the Reynolds number for all the tested configurations. Values obtained for the rectangular channel with flat surfaces, operated at the same conditions, are also plotted for comparison.

For the smooth rectangular-channel, the average Nusselt number remains nearly a constant for Reynolds numbers up to 2100, then it starts to increase exhibiting a power-law dependence on Re with an exponent of about 0.8. The figure also reports as solid lines the values Nu_0 calculated for a smooth rectangular-channel by the Shah and London correlation with Wibulsas correction for Re<2300, and by the Gnielinski correlation for Re>2300 [23]; all predictions take into account thermal effects of the entry-region. As it can be seen, the data agree very well with predictions.

For all the ribbed configurations, however, the average Nusselt number displays an increasing trend even from the minimum value of the investigated Reynolds numbers, revealing a power-law dependence on Re with an exponent ranging between 0.84 and 0.86. The lack of a constant Nu region induces to suppose that flow becomes turbulent at Re<700 in these channels. This seems to be confirmed by the trend of the friction factor that is almost constant in the whole range of the Reynolds number, as shown in figure 4b. For comparison, the figure also reports in solid line the values f_0 calculated for a laminar and turbulent flow through a smooth rectangular channel by means of Shah and London correlation [23]. Eventually, it is worthwhile noting that for Re<2000 the authors were unable to find in the open literature any data for ribbed channels for comparison.

As expected, the adoption of the ribbed surface determines an increase in both the Nusselt number and the friction factor for the same Reynolds number with respect to the smooth channel. The comparison is shown in figures 5a and 5b, respectively. In particular, it is seen that the enhancement factor Nu/Nu_0 (figure 5a) rapidly grows in the range 700<Re<3200, attaining a maximum at about Re=3200, then decreasing more slowly with an asymptotic tendency. The performance decays with the pitch-to-side ratio, and the maximum enhancements are 4.1, 3.4 and 2.4, respectively for p/e=10, 20 and 40. On the other hand, the penalization factor f/f_0 (figure 5b) shows a strong increase in the range 700<Re<3200, then it undergoes a flattened trend, where an initial decrease

is followed by a very weak rise. In this flattened range, corresponding to Re>3200, the penalization factor attains the maximum value, which results 15.3 ± 0.6 , 10.2 ± 0.6 and 5.6 ± 0.4 , respectively, for p/e=10, 20 and 40. Hence, in this case, the performance improves with the pitch-to-side ratio, but it is seen that the penalization factor is always greater than the enhancement factor. It is then very interesting from an engineering point of view to assess how these behaviors affect the overall performance accounting simultaneously for the effects on the heat transfer coefficient and the pressure drop. Among the various criteria adopted in the literature [2]-[16], [21], it is presented here the performance comparison at constant pumping power, which is synthesized in the index

$$\frac{Nu/Nu_0}{\left(f/f_0\right)^{1/3}}\tag{3}$$

plotted against the Reynolds number in figure 6. The behavior is quite similar to that of the enhancement factor. In particular, it is seen that the adoption of the ribbed surface seems not suitable for Re<1300, whereas it becomes more and more advantageous in the range 1300<Re<3200, where the index attains a maximum, followed by a slow decrease with an asymptotic trend. The dependence on the pitch-to-side ratio seems to be weaker than for the enhancement factor: the performance still decays with p/e but appreciable differences are noticed only for p/e=40.

Finally, the heat transfer data are summarized in the following correlation

$$Nu = 0.1213 \,\mathrm{Re}^{0.85} \,\mathrm{Pr}^{0.33} \left(\frac{p}{e}\right)^{-0.38}$$
 (4)

which fits the measurements with a relative error of 3.3%, and a coefficient of determination r^2 =0.9969.

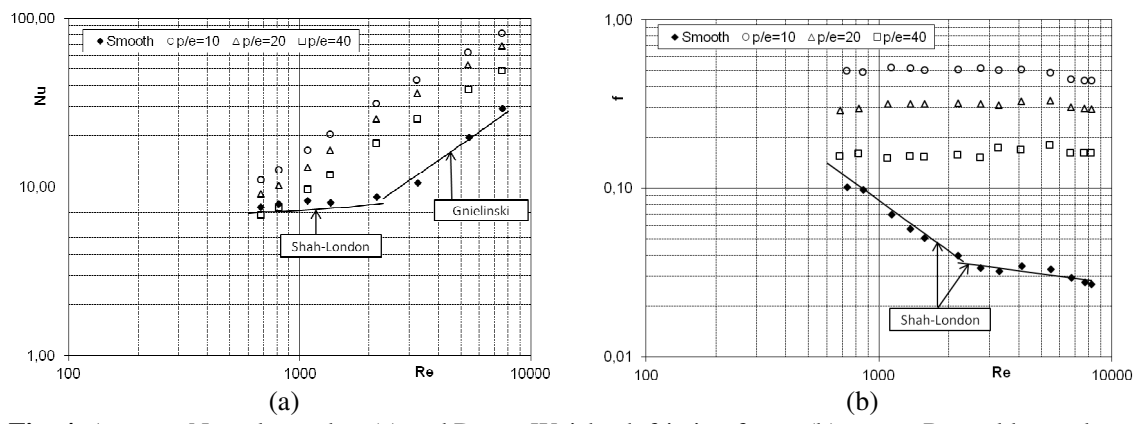


Fig. 4 Average Nusselt number (a) and Darcy-Weisbach friction factor (b) versus Reynolds number.

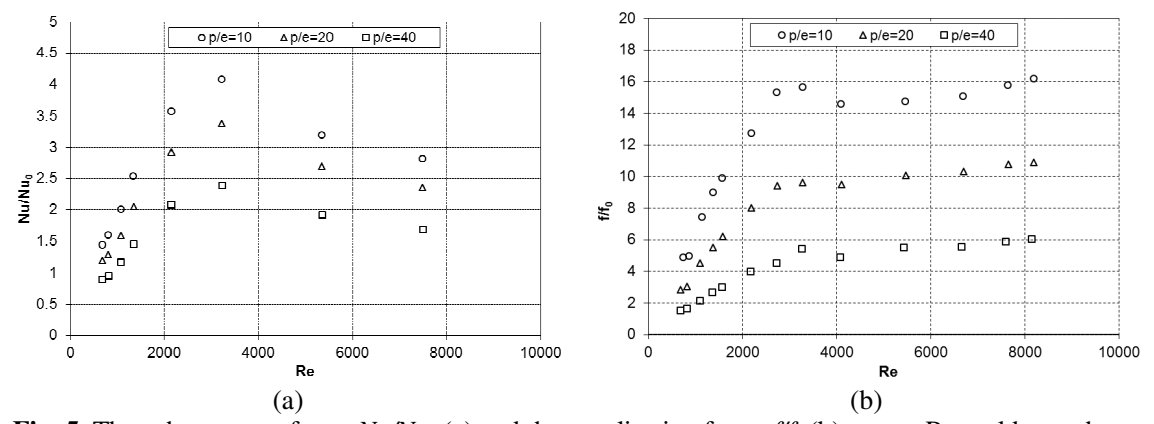


Fig. 5 The enhancement factor Nu/Nu_0 (a) and the penalization factor f/f_0 (b) versus Reynolds number.

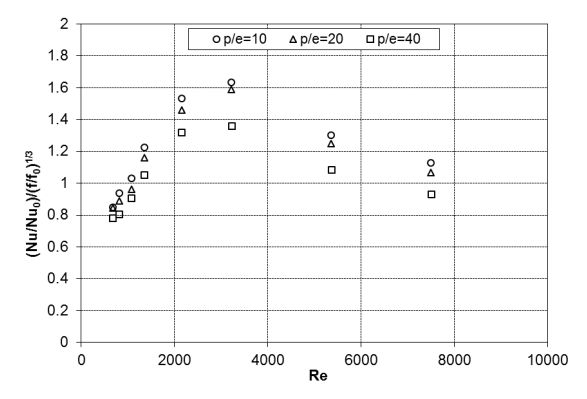


Fig. 6 The performance comparison at constant pumping power.

5. CONCLUSIONS

This paper reports an experimental investigation on heat transfer characteristics of a forced air-flow through a rectangular channel with the lower and upper surfaces roughened by V-shaped ribs (apex upward) with different pitch-to-side ratios (10, 20 and 40) at Reynolds numbers ranging between 700 and 7500. The enhancement effect compared to the smooth channel is due to both the periodic streamline deflection induced by the ribs, and the onset of turbulence at Re<700, as it can be induced by the growing trend of the average Nusselt number in the whole investigated range. The heat transfer data have been summarized in a Nu-Re correlation characterized by $\pm 3.3\%$ relative error, and a coefficient of determination r^2 =0.9969. To evaluate the overall performance, the Darcy-Weisbach friction factor has been reported as well, and the pressure drop penalization has been evaluated in comparison with the smooth channel. Even though the increase in the friction factor is always greater than the heat transfer enhancement, the performance index at constant pumping power reveals that it is convenient to adopt the ribbed surfaces for Re>1300, with an optimum at about Re=3200 for all the pitch-to-side ratios. On the other hand, the performance generally improves with decreasing values of p/e.

NOMENCLATURE

Symbol	Quantity	Unit
A	Channel cross section area	m^2
A_S	Channel total heated area	m^2
AR	Channel aspect ratio	-
c_p	Air specific heat at constant pressure	$J kg^{-1} K^{-1}$
\hat{D}_h	Channel hydraulic diameter	m
e	Rib side dimension	mm
f	Darcy-Weisbach friction factor	-
h	Channel height	mm
\overline{h}	Average convective coefficient	$W K^{-1} m^{-2}$
k	Air thermal conductivity	$W K^{-1} m^{-1}$
ℓ_{taps}	Distance between the pressure taps	m
m	Air mass flow-rate	kg s ⁻¹
Nu	Average Nusselt number	-
p	Rib pitch	mm
Δp	Pressure drop over ℓ_{taps}	Pa
Pr	Prandtl number	-
\dot{Q}	Total heat power exchanged	W
Re	Reynolds number	-
$\Delta T_{m,Log}$	Log-mean-temperature difference	K
\dot{V}	Air volume flow-rate	$m^{3} s^{-1}$
W	Channel width	mm

Greek symbols

Subscripts

i Inlet o Outlet

O Performance of smooth channel

REFERENCES

- [1] Gupta S., Chaube A. and Verma P., "Review on Heat Transfer Augmentation Techniques: Application in Gas Turbine Blade Internal Cooling", *J.Eng. Sci. Tech. Rev.*, 1, pp. 57-62, (2012).
- [2] Han J. C. and Park J. S., "Heat transfer enhancement in channels with turbulence promoters", *J. Eng. Gas Turb. Power*, 107, pp. 628-635, (1985).
- [3] Han J. C., "Heat transfer and friction characteristics in rectangular channel with rib turbulators", ASME J. Heat Trans., 110, pp. 321-328, (1988).
- [4] Han J. C. and Park J. S., "Developing heat transfer in rectangular channels with rib turbolators", *Int. J. Heat Mass Tran.*, 31, pp. 183-195, (1988).
- [5] Han J. C., Ou S., Park J. S. and Lei C. K., "Augmented heat transfer in rectangular channels of narrow aspect ratios with rib turbolators", *Int. J. Heat Mass Tran.*, 32, pp. 1619-1630, (1989).
- [6] Han J. C. and Zhang Y. M., "Effect of Rib-Angle Orientation on Local Mass Transfer Distribution in a Three-Pass Rib-Roughened Channel", *J. Turbomach.*, 113, pp. 123-130, (1991).
- [7] Han J. C., Zhang Y. M. and Lee C. P., "Augmented heat transfer in square channels with parallel, crossed, and V-shaped angled ribs", *J. Heat Trans.*, 113, pp. 590-596, (1991).
- [8] Park J. S., Han J. C., Huang Y., Ou S. and Boyle R. J., "Heat transfer performance comparisons of five different rectangular channels with parallel angled ribs", Int. J. Heat Mass Tran., 35, pp. 2891-2903, (1992).
- [9] Kukreja R. T., Lau S. C. and McMillin R. D., "Local heat/mass transfer distribution in a square channel with full and V-shaped ribs", *Int. J. Heat Mass Tran*, 36, pp. 2013-2020, (1993).
- [10] Liu J., Gao J. and Gao T., "Forced convection heat transfer of steam in a square ribbed channel", J. Mec. Sci. Tech., 4, pp. 1291-1298, (2012).
- [11] Liu J., Gao J., Gao T. and Shi X., "Heat transfer characteristics in steam-cooled rectangular channels with two opposite ribroughened walls, *App. Therm. Eng.*, 50, pp. 104-111, (2013).
- [12] Choi E Y, Choi Y .D, Lee W S, Chung J T and Kwak J S, "Heat transfer augmentation using rib-dimple compound cooling technique", *App. Therm. Eng.*, 51, pp. 435-441, (2013).
- [13] Smulsky Y. I., Terekhov V. I. and Yarygina N. I., "Heat transfer in turbulent separated flow behind a rib on the surface of square channel at different orientation angles relative to flow direction", *Int. J. Heat Mass Tran.*, 55, pp. 726-733, (2012).
- [14] Tanda, G., "Effect of rib spacing on heat transfer and friction in a rectangular channel with 45° angled rib turbulators on one/two walls", Int. J. Heat Mass Tran, 54, pp. 1081-1090, (2011).
- [15] Won S. Y. and Ligrani P. M., "Comparisons of flow structure and local Nusselt numbers in channels with parallel- and crossed-rib turbulators", *Int. J. Heat Mass Tran.*, 47, pp. 1573-1586, (2004).
- [16] Gao X. and Sunden B., "Heat transfer and pressure drop measurements in rib-roughened rectangular ducts", *Exp. Therm. Fluid Sci.*, 24, pp. 25-34, (2001).
- [17] Tanda, G., "Performance of solar air heater ducts with different types of ribs on the absorber plate", Energy ,36 (11), pp. 6651-6660, (2011).
- [18] Bhushan B. and Singh R., "A review on methodology of artificial roughness used in duct of solar air heaters", *Energy*, 35, pp. 202-212. (2010).
- [19] Hans V. S., Saini R. P. and Saini J. S., "Heat transfer and friction factor correlations for a solar air heater duct roughened artificially with multiple V-ribs", *Sol. Energy*, 84, pp. 898-911, (2010).
- [20] Patil A K, Saini J S and Kumar K., "A Comprehensive Review on Roughness Geometries and Investigation Techniques Used in Artificially Roughened Solar Air Heaters", Int. J. Ren. Energy Res., 2, pp. 1-15, (2012).
- [21] Webb R. L., Principles of enhanced heat transfer, New York: Winley-Interscience, (1994).
- [22] Moffat R. J., "Describing the uncertainties in experimental results", Exp. Therm. Fluid Sci., 1, pp. 3-17, (1988).
- [23] Kakaç S., Shah R. K., Aung W., Handbook of single-phase convective heat transfer, New York: Wiley-Interscience, (1987).